Journal of Applied Polymer Science

Flexible X-ray radiation protection membrane PVA/pb$(NO_3)_2$ microcapsule composites supported by bacterial cellulose

Lian Tang, Yi Zheng, Shiyan Chen, Lei Wang, Huaping Wang

State Key Laboratory for Modification of Chemical Fibers and Polymer Materials, Key Laboratory of Textile Science & Technology (Ministry of Education), College of Materials Science and Engineering, Donghua University, Shanghai 201620, People's Republic of China

Correspondence to: S. Chen (E-mail: chensy@dhu.edu.cn) or H. Wang (E-mail: wanghp@dhu.edu.cn)

ABSTRACT: Flexible and nonpoisonous X-ray-shielding membranes supported by bacterial cellulose (BC) were prepared, in which X-ray-shielding materials were of microcapsule structure by using polyvinyl alcohol as shell and lead salt as core. The effect of the wall/core interaction and the amount of cross-linking agent were taken into consideration to find the optimal reaction conditions. The morphology, microcapsule size, and lead salt release properties were investigated. After supported by BC, the flexible and potable membranes for X-ray radiation protection were prepared and the shielding properties were evaluated, which indicated a good X-ray-shielding material. We set up a new method to prepare flexible and portable X-ray radiation protection membranes. © 2015 Wiley Periodicals, Inc. J. Appl. Polym. Sci. **2016**, *133*, 43120.

KEYWORDS: biomaterials; composites; X-ray

Received 14 August 2015; accepted 31 October 2015
DOI: 10.1002/app.43120

INTRODUCTION

X-ray, an electromagnetic radiation with large penetration capability, is widely used in medical diagnosis, medical treatment, imaging, and crystal research fields.[1–4] However, X-ray pollution is a kind of main electromagnetic radiation pollution which must be well-controlled. The research on electromagnetic radiation protection plays an important role in the area of radiation physics. The mechanism of electromagnetic radiation shielding is energy absorption, and the shielding effectiveness is in direct proportion to the fourth power of the atomic number. The atomic number of lead is 82, which means it has excellent energy absorption property.[5] Thus, lead is frequently used in X-ray shielding. However, lead plates are limited to stationary X-ray protection for their toxicity,[6] high price, and heavy weight.[7,8] Compared with lead plates, lead composite materials are much more flexible and light weighted. Among these, lead exists as the lead salt in the composites and thus there is a question of lead lost, which can be resolved by microcapsule technology. It is a kind of technology to form a core–shell structure by cladding solid or liquid with film forming materials. The core is isolated with the outside environment by the shell and is intact.[9] Microcapsule technology brings many advantages, such as reducing volatility of perfume or organic solvents and extending their preservation, preventing toxic substance from leaking.[10,11] Thus, the application of microcapsule is very extensive, such as medical science,[12] coating,[13] textile,[14] food product,[15] and so on. The shell materials of microcapsules can be classified into three types: natural polymer, half-synthetic polymer, and synthetic polymer. Among them, polyvinyl alcohol (PVA) is one of the most extensively used.[16–18] The density of microcapsule can be controlled through modeling the degree of cross-linking, which can adjust the release amount of the core material. Based on these characteristics, we can decrease the amount of lead release through increasing the compactness of microcapsule wall materials.

The matrix for the portable lead composites have been reported for many polymers such as polyethylene,[19] rubber,[20,21] resin,[22] and so on. However, it still has some pending chronic problems: frangibility and poor humidity resistance.[23] These problems limit the lead materials applying to portable X-ray protection materials. Bacterial cellulose (BC) is a kind of cellulose obtained from *Gluconacetobacter xylinus*. The chemical structure of BC is fundamentally the same as plant-based cellulose. Compared with plant-based cellulose, BC presents attractive characteristics, such as three-dimentional (3D) ultrafine nanofiber network structure (nanofibrils with diameters at around 30–100 nm), high crystallinity, high degree of polymerization, high chemical purity, high tensile strength, and excellent biocompatibility.[24–27]

Additional Supporting Information may be found in the online version of this article.

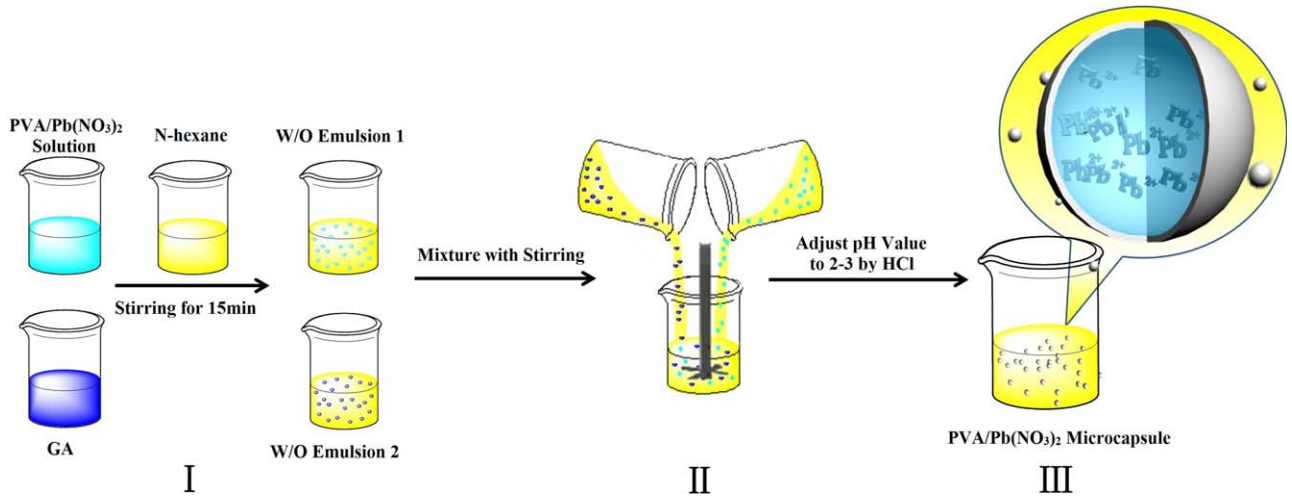

Figure 1. The schematic illustration for the formation process of PVA/$Pb(NO_3)_2$ microcapsules. [Color figure can be viewed in the online issue, which is available at wileyonlinelibrary.com.]

BC is also an excellent matrix material with abundant active hydroxyl, excellent moldability, and perfect performance during the formation. Due to the above features, researchers have done a plenty of investigations on BC-based composites such as PANI/BC,[27] PPy/BC,[28] CNT/BC,[29] Fe_3O_4/BC,[30] and so on.

BC and PVA have plenty of hydroxyl groups; PVA microcapsules fix on BC nanofibers uniformly through hydrogen bonds formed by these hydroxyl groups. Therefore, we plan to layout water-in-oil (W/O) structure microcapsules for X-ray protection by using PVA as shell and lead salt as core. The flexible and nonpoisonous X-ray-shielding membranes are obtained through composing the microcapsules and BC pulp. The effect of the wall/core interaction and the amount of cross-linking agent are taken into consideration to find the optimal reaction conditions. In addition, the morphology and lead salt release property of the microcapsules were investigated. Also, the X-ray-shielding performance and mechanical property of microcapsules/BC composite membranes were further studied.

EXPERIMENTAL

Materials and Characterization

Poly (vinyl alcohol) (PVA) ($M_w = 1750 \pm 50$), glutaraldehyde (GA) (25% w/v), Span-80, light petroleum, hydrochloric acid (HCl), and *n*-hexane were purchased from Shanghai Chem. Reagent Co. (China). Lead nitrate [$Pb(NO_3)_2$] was purchased from Aladdin Chemical Company Co., Ltd. BC was prepared in our laboratory.

The morphologies of membranes were observed using S-4800 field emission scanning electron microscope (FE-SEM). Transmission electron microscope (TEM) analysis was conducted using a JEM-2100 (JEOL, Japan) electron microscope operating at 200 kV. The MS 2000 laser particle size analyzer (Malvern, UK) was used to determine the average particle sizes and size distribution of microcapsules. The FT-infrared (FTIR) spectra of samples were recorded on a Nicolet NEXUS-670 FTIR. Inductively coupled plasma emission spectrometer (ICP) was performed on a Prodigy (Leeman, America) emission spectrometer to measure the content of lead salt in microcapsules and the lead salt release behavior. The thermal stability of the samples was measured by the TG 209 F1 Iris Thermogravimetric Analyzer. Tensile strengths of the heat-dried membranes were measured at room temperature using a WDW 3020 Universal Testing Machine and with a speed of 2 mm/min. X-ray-shielding performance of the membranes was recorded on an X'mind D03110 Dental X-ray machine.

Fabrication of PVA/$Pb(NO_3)_2$ Microcapsules

PVA/$Pb(NO_3)_2$ microcapsules were synthesized by W/O inverse miniemulsion process. PVA was chemically cross-linked with GA as the wall of the microcapsules, meanwhile the $Pb(NO_3)_2$ as the core would endow microcapsules shielding function.

The schematic process for the formation process of PVA/$Pb(NO_3)_2$ microcapsules is shown in Figure 1. First, PVA was dissolved in distilled water under 90°C and stirred for 3 h to form 5 wt % PVA solution. After cooling down to room temperature, different amounts of $Pb(NO_3)_2$ (0%, 2.5%, 5%, and 15% w/v, relative to PVA solution) were added to 100 mL 5 wt % PVA solution under constant stirring. Thereafter, 10 mL PVA/$Pb(NO_3)_2$ solution and 100 mL *n*-hexane (oil phase) were mixed with different amount of GA (0.25%, 2%, and 5% v/v, relative to PVA/$Pb(NO_3)_2$ and *n*-hexane solution), respectively, under stirring for 15 min to get W/O emulsion 1 and W/O emulsion 2. To maintain the stability of W/O emulsion and prevent the agglomeration of drops, 1% v/v Span-80, a nonionic surface-active agent which widely used in water-in-oil (W/O) reverse microemulsion, should be loaded into oil phase before water phase being mixed in. Then the inverse miniemulsion was prepared by mixing W/O emulsion 1 and W/O emulsion 2 with Ultra-Turrax® T25 homogenizer (IKA®, Germany) at 10,000 rpm for 30 min. HCl solution was added to initiate the interfacial polymerization between PVA and GA at oil water contact and stirring was continued for 30 min to form the microcapsules with uniform size and shape. Finally, the PVA/$Pb(NO_3)_2$ microcapsules were collected by centrifugation, and washed by light petroleum and distilled water repeatedly to remove oil phase,

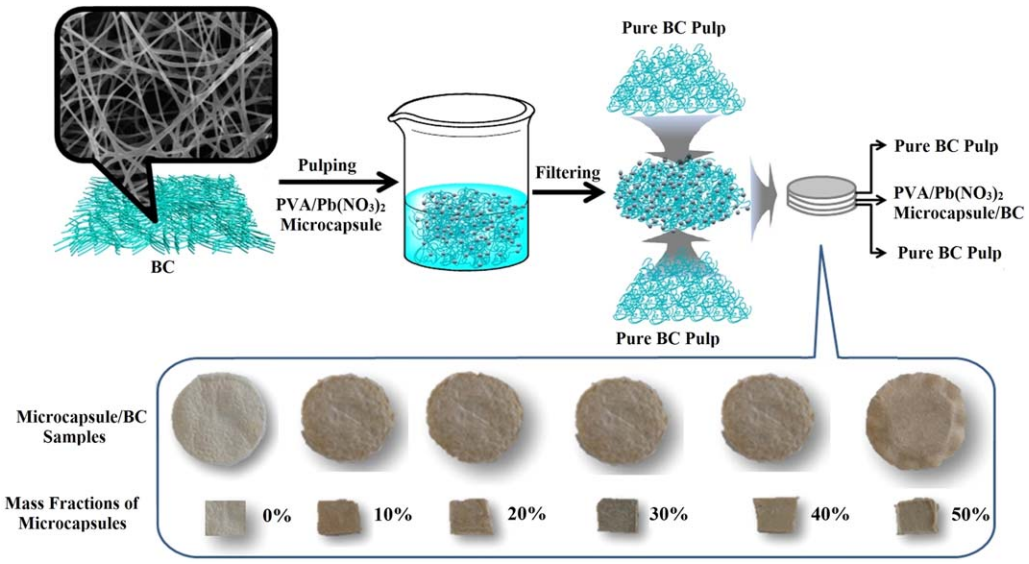

Figure 2. The schematic preparation process for microcapsule/BC composite membranes. [Color figure can be viewed in the online issue, which is available at wileyonlinelibrary.com.]

excess amount of surface-active agent, and unreacted GA. Then, the microcapsules were obtained after freeze-dried for 24 h.

Preparation of Microcapsules/BC Composite Membrane

As shown in Figure 2, the microcapsule/BC composite membranes were prepared by pulping and filtering. First, BC membranes were smashed by homogenizer and then formed BC pulp. Afterward, microcapsules were added into BC pulp under velocity mixing. Filtration process was used for film forming. In order to improve the safety of microcapsule/BC composite, pure BC pulp, microcapsule/BC composite pulp, and pure BC pulp were added in turn to fabricate a "sandwich" structure. After filtration, the composites were dried at 50°C.

Lead Salt Release Behavior

The release behavior measurement was performed by a conventional method. Two grams of microcapsule of different samples was spread into 10 g distilled water to prepare microcapsule suspensions. Then the suspension was placed for a certain time at 25°C. The release curve was determined by measuring the lead content in supernatant through ICP as a function of time.

The X-ray-Shielding Performance of Microcapsule/BC Composite Membranes Evaluation

To characterize the X-ray-shielding performance, aluminum (Al) equivalent-grayscale curve should be standardized before analyzing. Different thickness of Al sheets (1–10 mm, sampling interval was 1 mm) were placed into an X-ray machine and irradiated by X-ray with intensity of 8 mA. The distance between samples and photosource was 100 mm, and the exposure time was 0.125 s. After irradiating by X-ray, a series of X-ray pictures were obtained. As shown in Supporting Information, Figure S1 and Table S1, the worse the X-ray-shielding performance, the lower the value of gray. We can acquire the standard Al equivalent-gray curve using these data (Supporting Information, Figure S2). Supporting Information Figure S2 can help us to calculate the Al equivalent through the gray of microcapsule/BC composite membranes which can gain from X-ray pictures.

RESULTS AND DISCUSSION

Preparation Process for the PVA/$Pb(NO_3)_2$ Microcapsules

The preparation of PVA/$Pb(NO_3)_2$ microcapsules through W/O inverse miniemulsion is using the acetal membrane, which is formed by cross-linking PVA and GA to clad salt. There are two types of droplets in this system: $Pb(NO_3)_2$ droplet and GA droplet. $Pb(NO_3)_2$ and PVA are dispersed in *n*-hexane, span-80 as dispersant. When the pH of system is adjusted to 2–3, $Pb(NO_3)_2$ droplet and GA droplet cross-link on the W/O interface.[31]

The cross-linking reaction process is as shown in Scheme 1: the carbonyl in GA is attacked by hydrogen ion and formed a carbocation, and then one hydrogen ion of the hydroxy in PVA is taken by nucleophilic attack. Acetal reaction between PVA and GA can be triggered both inter-and intramolecularly.

Morphology and Structure of the Microcapsules

Figure 3 shows the FE-SEM images of PVA/$Pb(NO_3)_2$ microcapsules with different wall/core radio ($R_{w/c}$), respectively. From

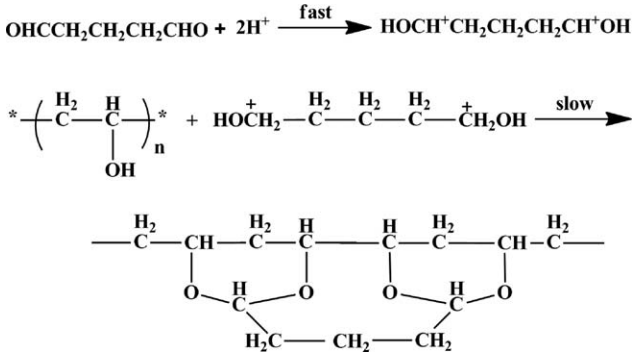

Scheme 1. The cross-linking reaction between PVA and GA.

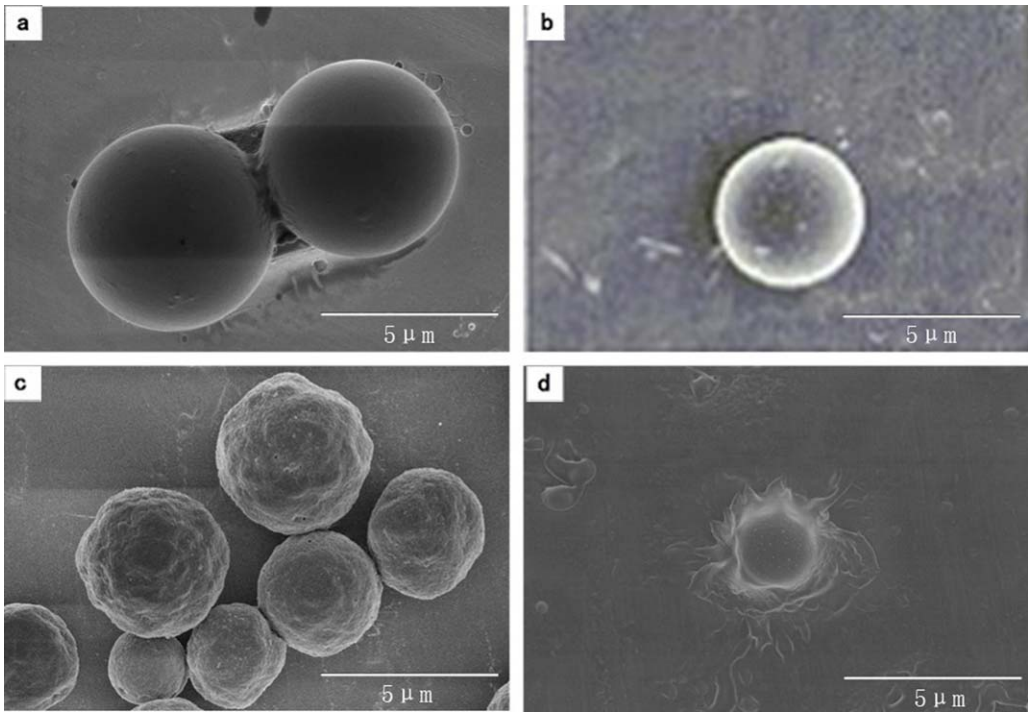

Figure 3. FE-SEM images of microcapsules with different wall/core radio ($R_{w/c}$), respectively: (a) PVA:$Pb(NO_3)_2$ = 5:0, (b) PVA:$Pb(NO_3)_2$ = 5:2.5, (c) PVA:$Pb(NO_3)_2$ = 5:5, (d) PVA:$Pb(NO_3)_2$ = 5:15. [Color figure can be viewed in the online issue, which is available at wileyonlinelibrary.com.]

Figure 3(a), we can see that the PVA microcapsules without $Pb(NO_3)_2$ have uniform and spherical shape with an average size mainly around 5 μm. Furthermore, the surface of PVA microcapsules are smooth and dense, which were not affected by the crystallization progresses of $Pb(NO_3)_2$ during the formation process. With the decrease of $R_{w/c}$, the morphology of microcapsules turns from spherical to irregular, and the surface of the microcapsules become rough and porous which can be seen from Figure 3(b,c). While the $R_{w/c}$ rises to 5:15, the microcapsule bursts. Therefore, the $R_{w/c}$ is the determining factor for the morphology and structure of the microcapsules. The excessive addition of $Pb(NO_3)_2$ would hinder the cross-linking between PVA and GA, thus result in forming rough, porous surface, even explosion of the wall [Figures 3(d) and 4(d)].

The TEM images of the microcapsules with and without $Pb(NO_3)_2$ are shown in Figure 4. As shown in Figure 4(a), the microcapsules without $Pb(NO_3)_2$ have a homogeneous structure; by contrast, the microcapsule with $R_{w/c}$ = 5:2.5 [Figure 4(b)] has an obvious core–shell structure and the thickness of wall is around 50 nm. $Pb(NO_3)_2$ is well coated by the microcapsules with modest $R_{w/c}$ prepared via inverse miniemulsion technique. After increasing the $Pb(NO_3)_2$ amount, $Pb(NO_3)_2$ would escape from the microcapsules [Figure 4(c,d)] because of the high porosity caused by the low $R_{w/c}$.

FTIR Spectroscopy

Figure 5 shows the FTIR spectra of pure PVA [Figure 5(a)] and PVA/$Pb(NO_3)_2$ microcapsules [Figure 5(b,c)]. The characteristic band of pure PVA at 2940 cm^{-1} refers to the stretching C–H from alkyl groups. The large bands between 3300 and 3500 cm^{-1} correspond to the stretching vibration of hydroxyl groups. Compared to pure PVA, the peak belonged to hydroxyl groups in PVA/$Pb(NO_3)_2$ microcapsules weaken due to the reaction of the PVA with GA, which consumed a lot of hydroxyl of PVA to form acetal bridges. The FTIR spectrum of PVA microcapsules reveals another band around 2860 cm^{-1} of C–H stretching related to aldehydes, which attributed to the alkyl chain.[16,32] In comparison with the PVA and microcapsule samples, the FTIR spectra of the two microcapsule samples have a sharp absorption peak at 1725 cm^{-1}, caused by the strong vibration of the C═O bond, indicating the presence of hemiacetal structure.[33] Therefore, the results of FTIR show the formation of the acetal bridges between hydroxyl groups by interfacial polymerization.

Release Evaluation of Microcapsule in Aqueous Medium

The additive amount of cross-linking agent is an important factor to the shielding property and safety of microcapsules.[34] Figure 6 shows the Pb content in microcapsules at various $R_{w/c}$ and GA amount. With the decrease of $R_{w/c}$ from 5:2.5 to 5:5, the Pb contents of different samples increase. However, when $R_{w/c}$ further decreased to 5:15, the Pb contents in the microcapsules decreased. It is because the wall structure would be damaged by overmuch $Pb(NO_3)_2$ crystal which would result in the leakage of lead. The result can be confirmed by the SEM and TEM discussed above. Moreover, from Figure 6, we can observe that the Pb content have not changed obviously with different the GA amount. Figure 7 shows the release curves of PVA/$Pb(NO_3)_2$ microcapsules with different GA addition in the aqueous medium. From the three curves shown in Figure 7, we can find that the release of lead salt from PVA/$Pb(NO_3)_2$ microcapsules exhibits three different phases[35]: (i) Volume expansion: The hydrophilic polymers PVA-GA with cross-linking structure

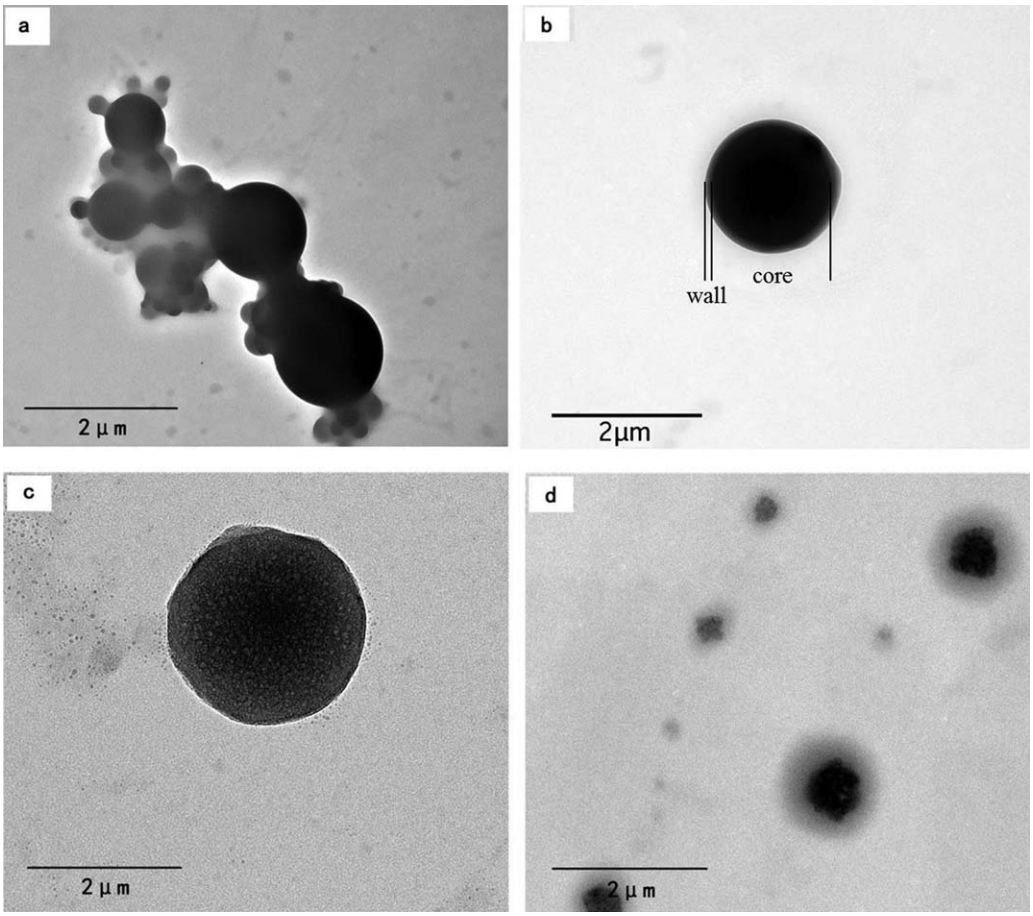

Figure 4. TEM images of microcapsules with different wall/core radio ($R_{w/c}$), respectively: (a) PVA:$Pb(NO_3)_2$ = 5:0, (b) PVA:$Pb(NO_3)_2$ = 5:2.5, (c) PVA:$Pb(NO_3)_2$ = 5:5, (d) PVA:$Pb(NO_3)_2$ = 5:15.

would be hydrated which leads to the relaxation of polymer chain. (ii) Accelerating release: The volume expansion causes the size of porous network increase, which allows more Pb^{2+} pass the wall. (iii) Release balance: A release–absorb balance establishes between microcapsules and the environment around them after a period of release time. For the lowest degree of cross-linking of GA in curve *a* which allows more Pb^{2+} to pass the wall and leak, the shortest time for volume expansion, the highest accelerating release rate, and the largest cumulative

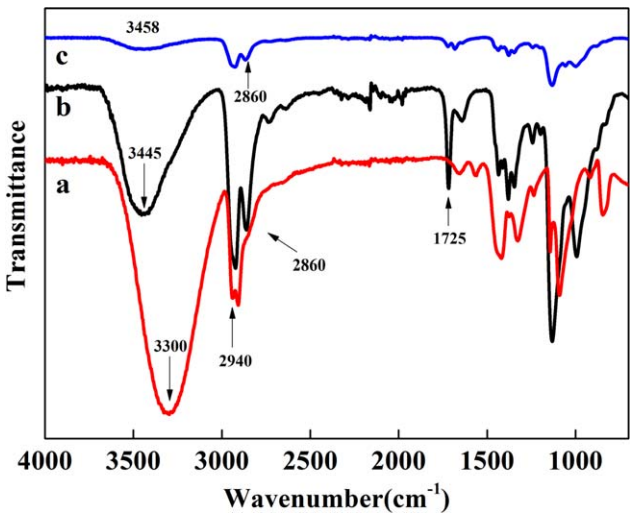

Figure 5. FTIR spectra of (a) PVA, (b) PVA/$Pb(NO_3)_2$ microcapsules $R_{w/c}$ = 5:0, and (c) $R_{w/c}$ = 5:2.5. [Color figure can be viewed in the online issue, which is available at wileyonlinelibrary.com.]

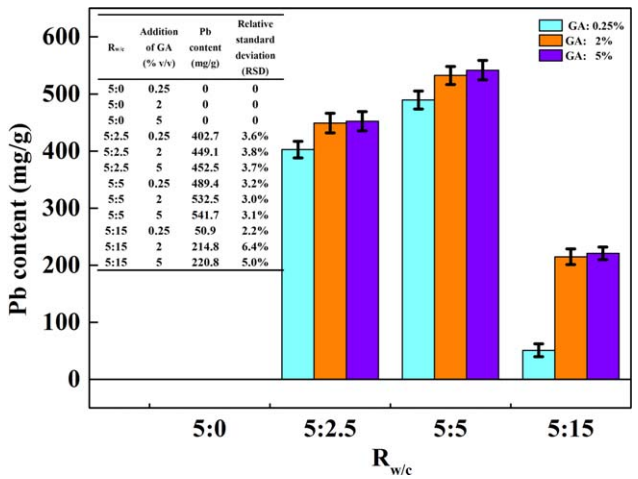

Figure 6. The Pb content of microcapsules with different $R_{w/c}$ and GA addition. The inset shows the data of Pb content. [Color figure can be viewed in the online issue, which is available at wileyonlinelibrary.com.]

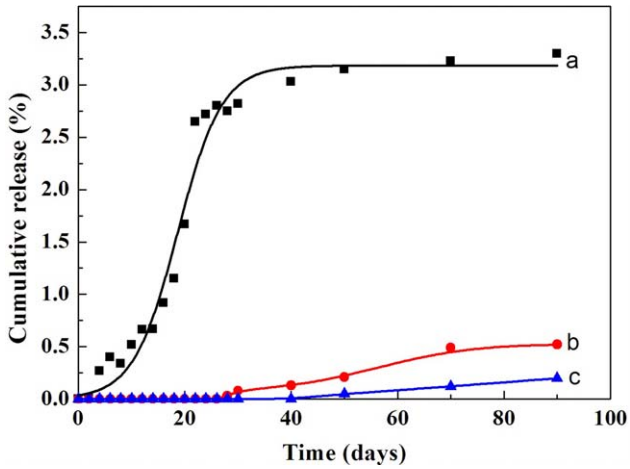

Figure 7. Diffusion of Pb^{2+} from microcapsules with different GA addition in the aqueous medium as a function of release time (a) 0.25%, (b) 2%, and (c) 5%. [Color figure can be viewed in the online issue, which is available at wileyonlinelibrary.com.]

release amount were observed. There is no obvious difference between curve *b* and curve *c* for most of the cross-linking reactions have been completed when the additive amount of GA is more than 2%. The cumulative release in 90 days is only 0.52% and 0.2% corresponding to the additive amount of GA is 2% and 5%, indicating the safety of PVA/$Pb(NO_3)_2$ microcapsules.

X-ray-Shielding Performance of Microcapsule/BC Composite Membranes

The X-ray-shielding performance of microcapsule/BC composite membranes was evaluated by aluminum (Al) equivalent-grayscale curve. Figure 8 reveals the aluminum (Al) equivalent-grayscale curve and X-ray-shielding performance of microcapsule/BC composites, the inset is the corresponding X-ray images of samples. As shown in Figure 8, the Al equivalent of pure BC with the thickness of 1 mm was 0.39 mm, which indicates that

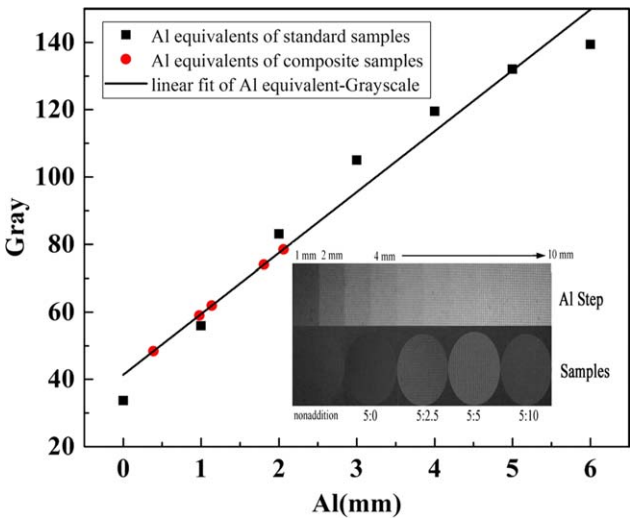

Figure 8. X-ray-shielding performance of microcapsule/BC composites; the inset is the X-ray images of samples. [Color figure can be viewed in the online issue, which is available at wileyonlinelibrary.com.]

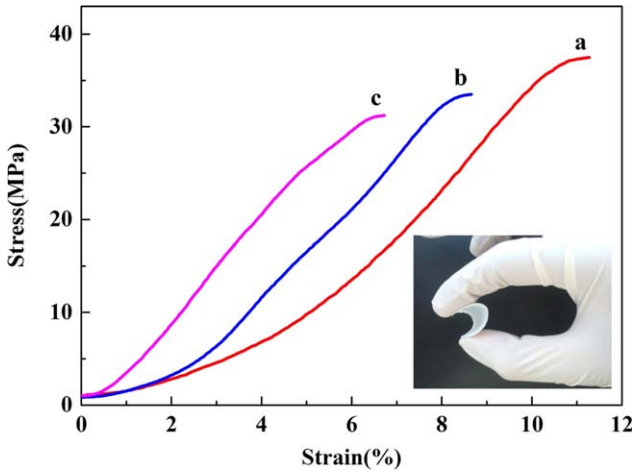

Figure 9. Strain–stress curves of pure BC (a) and microcapsule/BC composite membranes with different mass fractions of microcapsule (b) 30% and (c) 50%. The inset shows the optical image of microcapsule/BC composite membranes (50%). [Color figure can be viewed in the online issue, which is available at wileyonlinelibrary.com.]

pure BC have no X-ray-shielding effect. The Al equivalents of microcapsule/BC composites increase with the amount of microcapsules increase. The Al equivalents of composites rise to 0.98, 1.14, 1.81, and 2.06 mm when the mass fractions of microcapsules come to 20, 30, 40, and 50 wt %, respectively. According to the protection standard of dental, portable X-ray machine, composite materials with 1 mm Al equivalent can be used as individual protection. It means that when the amount of microcapsules surpass 20 wt %, microcapsule/BC composite membranes have an eligible X-ray-shielding performance.

Mechanical Property

To investigate the mechanical characteristics of microcapsule/BC membranes, the tensile test was performed. Figure 9 shows the strain–stress curves of pure BC and microcapsule/BC composite membranes with different mass fractions of microcapsule. Excellent mechanical property with tensile strength and elongation of 37.5 MPa and 11.3% for pure BC is observed, while the tensile strength and elongation for the microcapsule/BC composite with 50 wt % microcapsule decrease to around 31.2 MPa and 6.7%, respectively. This decreased behavior may associate with formation of the stress concentrative points in membranes caused by adding microcapsules to the system.[30] The inset shows the excellent flexibility of microcapsule/BC composite membrane, which means an advantage to applying in individual protection. It is obvious that the membranes combine the excellent mechanical properties of BC membrane and the X-ray shielding properties of the microcapsule indicating a promising material in the medical protective textile, portable protective field.

CONCLUSION

We have successfully prepared PVA/$Pb(NO_3)_2$ microcapsules by W/O inverse miniemulsion process. The lead salts were covered by PVA and formed a core–shell structure. The FTIR curves indicated formation of acetal bridges between PVA and GA

though the interfacial polymerization. When PVA/$Pb(NO_3)_2$ microcapsules was 5:2.5, additive span 80 amount was 1% and the additive GA amount was 2%, the morphology of the microcapsules was uniform spheres with the highest Pb content and the safe release. Further, flexible microcapsule/BC composite membranes were fabricated. The result showed that the Al equivalent of microcapsule/BC composite membranes was >1 when the content of microcapsule was over 20 wt %. In addition, microcapsule/BC composite membranes demonstrated an excellent flexibility and mechanical properties with tensile strength of 37.5 MPa. This work provides a straightforward method to prepare flexible membranes with high X-ray-shielding effectiveness, satisfactory security, and good mechanical properties, which endow the membranes potential applications in individual protection field.

ACKNOWLEDGMENTS

This work was financially supported by Program of Introducing Talents of Discipline to Universities (B07024), Shanghai Leading Academic Discipline Project (B603), The National Natural Science Foundation of China (51273043), Project of the Action on Scientists and Engineers to Serve Enterprises (2009GJE20016).

REFERENCES

1. Zhou, S. A.; Brahme, A. *Phys. Medica* **2008**, *24*, 129.
2. Lu, Y.; Xue, L. *Compos. Sci. Technol.* **2012**, *72*, 828.
3. Jacobs, P.; Sevens, E.; Kunnen, M. *Sci. Total Environ.* **1995**, *167*, 161.
4. Goldstein, L.; Prasher, S. O.; Ghoshal, S. *J. Contam. Hydrol.* **2007**, *93*, 96.
5. Prasad, S. G.; Parthasaradhi, K.; Bloomer, W. D.; Al-Najjar, W. H.; McMahon, J.; Thomson, O. *Radiat. Phys. Chem.* **1998**, *53*, 361.
6. Nambiar, S.; Osei, E. K.; Yeow, J. T. W. *J. Appl. Polym. Sci.* **2013**, *127*, 4939.
7. Kurudirek, M. *Nucl. Eng. Des.* **2014**, *280*, 440.
8. Zhai, W.; Chen, Y.; Ling, J.; Wen, B.; Kim, Y. W. *J. Cell Plast.* **2014**, *50*, 537.
9. Mirabedini, S. M.; Dutil, I.; Farnood, R. R. *Colloid. Surf. A* **2012**, *394*, 74.
10. Yun, J.; Im, J. S.; Lee, Y. S.; Kim, H. I. *Eur. Polym. J.* **2010**, *46*, 900.
11. Shchukina, E. M.; Shchukin, D. G. *Adv. Drug Deliver. Rev.* **2011**, *63*, 837.
12. Lam, K. H.; Cheng, S. Y.; Lam, P. L.; Yuen, C. W. M.; Wong, R. S. M.; Lau, F. Y.; Lai, P. B. S.; Gambari, R.; Chui, C. H. *Minerva Biotechnol.* **2010**, *22*, 23.
13. Xu, X. Q.; Guo, Y. H.; Li, W. P.; Zhu, L. Q. *Int. J. Min. Met. Mater.* **2011**, *18*, 377.
14. Feng, Q. Q.; Shen, L. P.; Li, D. M. *Appl. Mech. Mater.* **2012**, *184185*, 1124.
15. Kuang, S. S.; Oliveira, J. C.; Crean, A. M. *Crit. Rev. Food Sci.* **2010**, *50*, 951.
16. Seunguk, P. *Mater. Sci. Forum* **2006**, *510*. 678.
17. Li, J. K.; Wang, N.; Wu, X. S. *J. Control. Release* **1998**, *56*, 117.
18. Ossipov, D. A.; Hilborn, J. *Macromolecules* **2006**, *39*, 1709.
19. Durante, M.; George, K.; Gialanella, G.; Grossi, G.; La Tessa, C.; Manti, L.; Miller, J.; Pugliese, M.; Scampoli, R.; Cucinotta, E. A. *Radiat. Res.* **2005**, *614*, 571.
20. Kusiak, E.; Zaborski, M.; Staniszewska, M. A.; Bem, H.; Szajerski, P.; Baryn, W. *Polimery* **2013**, *58*, 519.
21. Ramakrishna, R.; Godkhindi, M. M.; Chakraborty, M.; Nanda, G. B. *Mater. Sci. Technol.* **1986**, *22*, 768.
22. An, J.; Wu, H.; Xin, Y. *J. Eng. Plast. Appl.* **2004**, *32*, 14.
23. Zuguchi, M.; Chida, K.; Taura, M.; Inaba, Y.; Ebata, A.; Yamada, S. *Radiat. Prot. Dosim.* **2008**, *131*, 531.
24. da Silva, A.; Nievola, L. M.; Tischer, C. A.; Mali, S.; Faria-Tischer, P. C. S. *J. Appl. Polym. Sci.* **2013**, *130*, 3043.
25. Hu, W.; Chen, S.; Yang, J.; Li, Z.; Wang, H. *Carbohyd. Polym.* **2014**, *101*, 1043.
26. Jorfi, M.; Foster, E. J. *J. Appl. Polym. Sci.* **2015**, DOI: 10.1002/app.41719.
27. Hu, W.; Chen, S.; Yang, Z.; Liu, L.; Wang, H. *J. Phys. Chem. B* **2011**, *115*, 8453.
28. Tang, L.; Han, J.; Jiang, Z.; Chen, S.; Wang, H. *Carbohyd. Polym.* **2015**, *117*, 230.
29. Yeseul, K.; Hun-Sik, K.; Hyeonseong, B.; Young Soo, Y.; Se Youn, C.; Hyoung-Joon, J. *J. Appl. Polym. Sci.* **2009**, *114*, 2864.
30. Zhang, W.; Chen, S.; Hu, W.; Zhou, B.; Yang, Z.; Yin, N.; Wang, H. *Carbohyd. Polym.* **2011**, *86*, 1760.
31. Yeom, C.; Oh, S.; Rhim, J.; Lee, J. *J. Appl. Polym. Sci.* **2000**, *78*, 1645.
32. Mansur, H. S.; Sadahira, C. M.; Souza, A. N.; Mansur, A. A. P. *Mat. Sci. Eng. C-Biomim.* **2008**, *28*, 539.
33. Hong, K. H.; Sun, G. *Polym. Eng. Sci.* **2010**, *50*, 1780.
34. Yeom, C.; Kim, Y.; Lee, J. *J. Appl. Polym. Sci.* **2002**, *84*, 1025.
35. Yun, J.; Kim, H. *J. Appl. Polym. Sci.* **2010**, *115*, 1853.